

$B_d \rightarrow K^{*0} \mu^+ \mu^-$ at LHCb

William Reece^{*†}

(on behalf of the LHCb collaboration)

E-mail: w.reece06@imperial.ac.uk

$\bar{B}_d \rightarrow \bar{K}^{*0} \mu^+ \mu^-$ is a rare electroweak $b \rightarrow s$ penguin decay that has excellent sensitivity to physics beyond the Standard Model. LHCb should collect 6200^{+1700}_{-1500} signal events with a residual background of 1550 ± 310 for each nominal year of data-taking. This allows for a comprehensive and exciting programme of physics measurements, the details of which will be reviewed in this article.

*12th International Conference on B-Physics at Hadron Machines - BEAUTY 2009
September 07 - 11 2009
Heidelberg, Germany*

*Speaker.

†Imperial College London

1. Introduction

As we enter the LHC era, we are confronted with the experimental fact that results from the Tevatron and the B -factories are, by and large, in agreement with Standard Model (SM) predictions. The working hypothesis of the LHC project is that there will be new physics (NP) at the TeV scale. However, considerations from flavour physics imply that the NP scale is much larger, assuming its flavour structure is generic. If these two observations are to be reconciled then the study of flavour will be of great interest at the LHC.

LHCb is a high precision experiment for the study of CP violation and rare decays at the LHC [1]. Of particular interest at LHCb will be the exclusive $b \rightarrow s$ decay mode $\bar{B}_d \rightarrow \bar{K}^{*0} \mu^+ \mu^-$. This is normally treated using the operator product expansion, where the Wilson coefficients $\mathcal{C}_{7,9,10}$ dominate. These have right-handed partners, $\mathcal{C}'_{7,9,10}$, that are highly suppressed in the SM and in minimal flavour-violating models. In the presence of NP, the values of these coefficients may change due to new heavy degrees of freedom in the loops. Measuring the Wilson coefficients then allows for entire classes of NP to be observed or excluded.

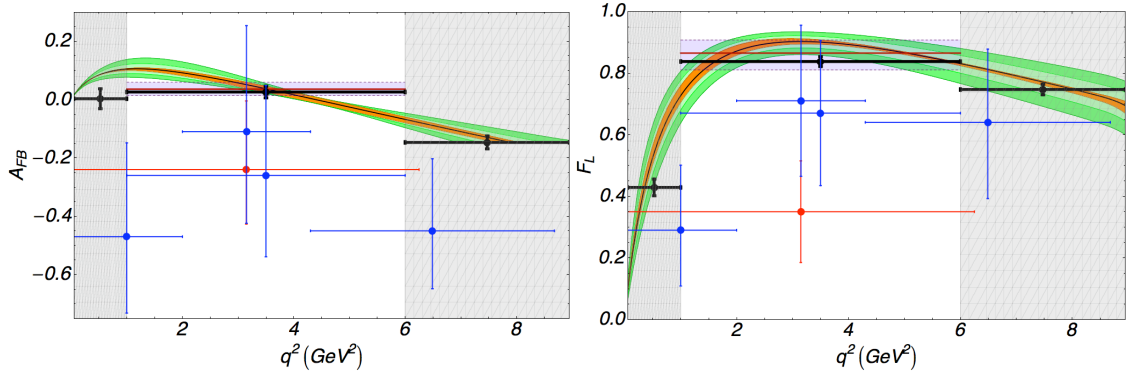


Figure 1: Recent results from *BABAR* (red) and *BELLE* (blue) for A_{FB} (left) and F_L (right) [2] (Figure author’s own). SM theoretical predictions are shown; the orange, light green, and dark green bands show the parametric and estimated 5% and 10% contributions from unknown higher order terms in the $1/m_b$ expansion, known as Λ/m_b corrections [3]. The light purple band shows the rate weighted SM average in the region $q^2 \in [1 \text{ GeV}^2/c^4, 6 \text{ GeV}^2/c^4]$, with all uncertainties. The black points show LHCb 2 fb^{-1} sensitivities using a simultaneous angular projection fit, following Ref. [4] and assuming the SM, where the central value is taken from a single toy experiment.

The kinematics of the decay is described by three angles, θ_l , θ_K , and ϕ , and the invariant mass squared of the $\mu\mu$ pair, q^2 . A widely studied observable is the di-lepton forward–backward asymmetry,

$$A_{FB}(q^2) = \frac{\int_0^1 \frac{\partial^2 \Gamma}{\partial q^2 \partial \cos \theta_l} d \cos \theta_l - \int_{-1}^0 \frac{\partial^2 \Gamma}{\partial q^2 \partial \cos \theta_l} d \cos \theta_l}{\int_0^1 \frac{\partial^2 \Gamma}{\partial q^2 \partial \cos \theta_l} d \cos \theta_l + \int_{-1}^0 \frac{\partial^2 \Gamma}{\partial q^2 \partial \cos \theta_l} d \cos \theta_l}. \quad (1.1)$$

The value of q^2 for which $A_{FB}(q^2)$ is 0, known as the zero–crossing point (q_0^2), has small theoretical uncertainties due to leading order form–factor (FF) cancellations [5]. The SM distribution can be seen in Fig. 1, however, the theoretical uncertainties are not well controlled outside of the $q^2 \in [1 \text{ GeV}^2/c^4, 6 \text{ GeV}^2/c^4]$ region [3; 6; 7]. Measurements from both *BABAR* and *BELLE* [2] are shown in Fig. 1 for points that lie inside this ‘theoretically clean’ region. Also shown is F_L , the longitudinal

polarisation fraction of the \bar{K}^* . The current experimental uncertainties are still too large to make any definitive statements about deviations from the SM and any differences seen are greatest outside of the theoretically clean q^2 region (not shown). The large increase in statistics from LHCb will clarify this situation. For comparison, the estimated sensitivities for LHCb with 2 fb^{-1} of integrated luminosity are shown in the same figure.

2. Physics Programme

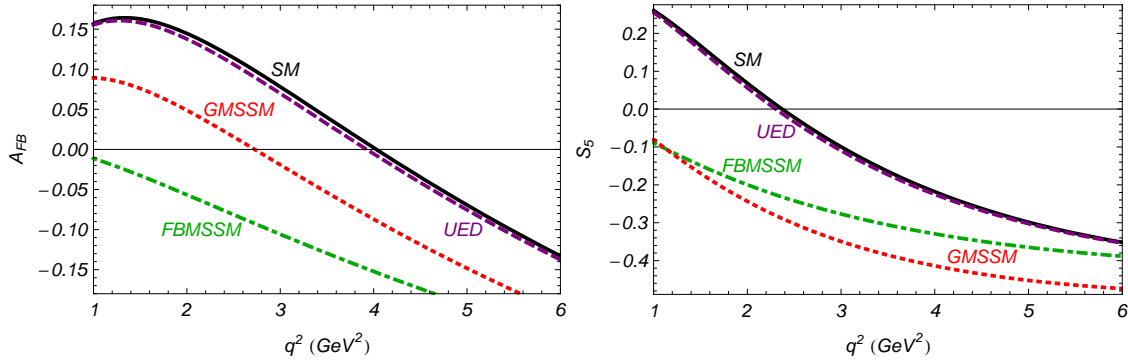


Figure 2: Theoretical A_{FB} and S_5 distributions in a number of models [8]. The solid lines give the SM prediction. The dashed lines show predictions from a universal extra dimensions (UED) model, a non-minimal flavour violating supersymmetric model (GMSSM) and a flavour blind supersymmetric model (FBMSSM). Details of these models can be found in [7].

Making precision B -physics measurements in the LHC environment will be challenging but LHCb has been carefully optimised to make this possible [1]. The detector is expected to collect $6200^{+1700}_{-1500} B_d \rightarrow K^{*0} \mu^+ \mu^-$ signal events with 1550 ± 310 background events for each nominal year of data-taking (2 fb^{-1}) [9]. The dominant uncertainty on this yield estimate comes from the branching fraction, which is currently known to an accuracy of $\sim 15\%$. The large increase in statistics at LHCb relative to the previous generation of experiments allows for an ambitious physics programme to be undertaken [10]. A selection of measurements of the angular distribution are discussed below.

2.1 Measuring A_{FB}

The first major analysis target is to map out the A_{FB} distribution and determine q_0^2 . This measurement can be made with relatively low integrated luminosity using a counting experiment in θ_l , as shown on the left of Fig. 3. Taking a particular FF model [11], this approach gives a projected uncertainty of $\sigma(q_0^2) = 0.46 \text{ GeV}^2/c^4$ for 2 fb^{-1} of integrated luminosity [12]. However the uncertainty is approximately proportional to the gradient of the A_{FB} distribution, which is in turn dependent on the FFs and indeed the physics model found in nature, meaning that the actual uncertainty found may differ from this (see the left-most graphic of Fig. 2).

A particular challenge of making this measurement will be dealing with detector and selection acceptance effects, particularly at low q^2 . While a measurement of q_0^2 should be safe from biases due to these, the rest of the A_{FB} distribution can see considerable warping, leading to a systematic

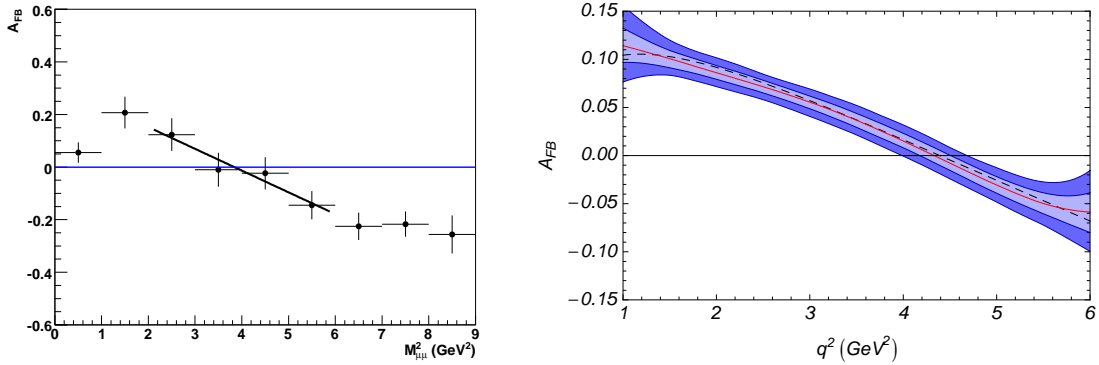


Figure 3: **Left:** A 2 fb^{-1} counting experiment, from Ref. [12], produced using the full LHCb detector simulation and a SM signal simulation following Ref. [11] ($M_{\mu\mu}^2 \equiv q^2$). A straight-line fit is used to extract q_0^2 . **Right:** Estimated sensitivity to A_{FB} in the range $q^2 \in [1 \text{ GeV}^2/c^4, 6 \text{ GeV}^2/c^4]$ as extracted using a full angular analysis to 10 fb^{-1} of toy LHCb data, with the SM signal simulation following Refs. [3; 6]. The dashed black line shows the input SM distribution, while the solid red line is the median of a thousand toy fits. The 1σ and 2σ confidence levels are marked by the light and dark blue bands. The differing input calculations and FF distributions lead to the variations in gradient and q_0^2 between the two figures.

effect on $\sigma(q_0^2)$ from the change in the A_{FB} gradient induced. These effects must be controlled to an accuracy of $\sim 10\%$ if their contribution to the final uncertainty is to be small. The left-most graphic in Fig. 4 shows the effects on the θ_l efficiency due to the LHCb detector geometry and reconstruction in the low q^2 region, $q^2 \in [1 \text{ GeV}^2/c^4, 2 \text{ GeV}^2/c^4]$. Many more events with θ_l close to 0 or π are lost than those with θ_l close to $\pi/2$. Events in the former configurations typically feature one high p_T and one low p_T muon; at low q^2 the lower momentum μ often fails to reach the muon chambers and is not reconstructed.

The events with $\theta_l \approx 0$ or π are particularly important for the A_{FB} analysis, as they will show the largest asymmetry in θ_l , and are expected to be produced much less frequently than those with $\theta_l \approx \pi/2$. The middle graphic of Fig. 4 shows the effect of introducing a $300 \text{ MeV } p_T$ cut on both muons. In this case the effect is disastrous, with the vast majority of these significant events lost. While these effects are less important at higher q^2 , considerable care must be taken to avoid producing these kind of effects in the theoretically clean region. The right-most graphic in Fig. 4 shows the current effect of the LHCb trigger and offline selections on a sample of fully simulated signal events. It can be seen that there is little extra warping introduced, and so the main source of acceptance effects is expected to be from the detector geometry and reconstruction.

2.2 Beyond A_{FB}

Counting experiments in θ_l are attractive as they require a relatively modest understanding of the detector and backgrounds. However, there is much more information available in the decay which can be extracted at the price of a more challenging analysis. These measurements are important as they are complementary to A_{FB} and provide sensitivity to Wilson coefficients beyond \mathcal{C}_7 and \mathcal{C}_9 . Projections of the full angular distribution can be used to perform a simultaneous fit to the decay angles [4]. This gives additional sensitivity to A_{FB} and F_L , shown in Fig. 1, and to

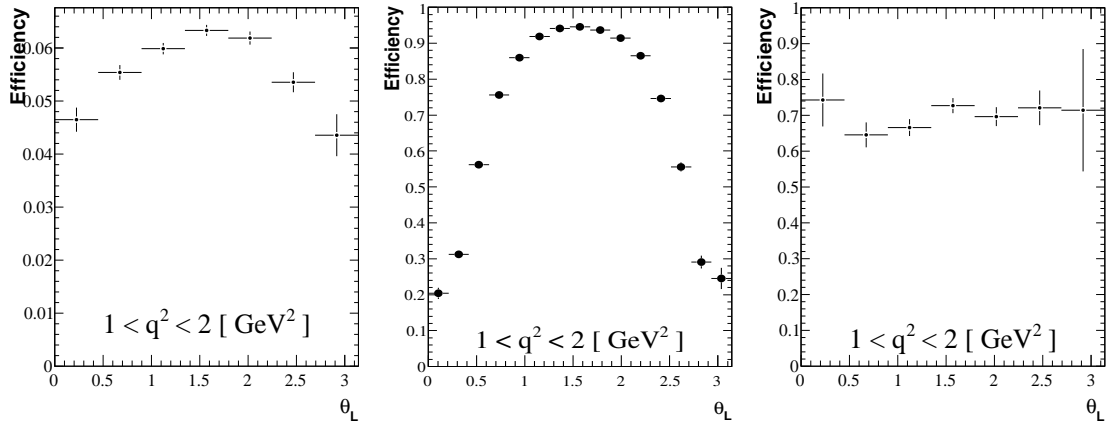


Figure 4: **Left:** The effect of the detector geometry and reconstruction on the signal selection efficiency as a function of θ_l found from a full detector simulation. **Middle:** The effect of requiring that both muons have a $p_T > 300$ MeV on the signal selection efficiency using a generator level simulation of the decay kinematics. **Right:** The total effect on the signal selection efficiency from the complete trigger chain, relative to the detector geometry and reconstruction effect, found from a full detector and trigger simulation.

non-SM values of \mathcal{C}'_7 via a new observable, $A_T^{(2)}$ [13]. Sensitivity to \mathcal{C}'_7 may also be gained via the observable S_5 [7], theoretical distributions for which are shown in Fig. 2. This also features a zero-crossing point, the measurement of which may be attractive experimentally due to the steep gradient at this point for SM like scenarios [8]. Like A_{FB} , S_5 may be extracted with a counting experiment using the expression

$$S_5 = \frac{4}{3} \left[\int_0^{\pi/2} + \int_{3\pi/2}^{2\pi} - \int_{\pi/2}^{3\pi/2} \right] \partial\phi \left[\int_0^1 - \int_{-1}^0 \right] \partial \cos \theta_K \frac{\partial^3 \Gamma}{\partial q^2 \partial \phi \partial \cos \theta_K} / \frac{\partial \Gamma}{\partial q^2}, \quad (2.1)$$

however controlling acceptance effects in the two angles will be a challenge.

Finally, it is possible to perform a full angular analysis [3]. In this case all four experimental observables are utilised to extract the underlying decay amplitudes. This allows for the measurement of additional observables which cannot be accessed in other ways. Fig. 5 shows the estimated LHCb sensitivity to the theoretically clean observables $A_T^{(3)}$ and $A_T^{(4)}$ for a simulated 10 fb^{-1} data set. In addition, significant improvement can be gained on A_{FB} and q_0^2 . The right-hand figure of Fig. 3 shows the expected sensitivity to A_{FB} with 10 fb^{-1} of integrated luminosity, giving $\sigma(q_0^2) = {}^{+0.18}_{-0.16} \text{ GeV}^2/c^4$. A further factor of ~ 2 improvement might be expected if the FF model from [11] had been used instead of that from [6].

2.3 CP Violation

LHCb reconstructs $\bar{B}_d \rightarrow \bar{K}^{*0} \mu^+ \mu^-$ through the charged decays of the \bar{K}^{*0} so the sign of the K tags the B flavour. Both model dependent [7] and model independent [14] considerations indicate that significant non-SM like CP violation is possible in the decay though the addition of complex phases in the Wilson coefficients. These remain poorly constrained and could in principle provide a source of CP violation beyond the CKM mechanism. The SM contribution is very small, coming from doubly-Cabibbo suppressed diagrams, and so any CP violation in this decay would be a

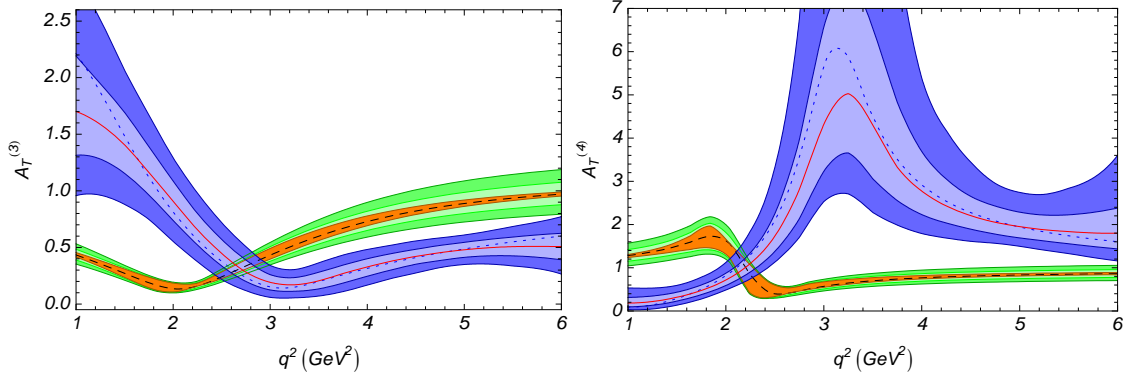


Figure 5: Experimental sensitivity bands (1σ and 2σ uncertainties are marked light and dark blue) compared to the theoretically clean observables $A_T^{(3)}$ and $A_T^{(4)}$ for 10 fb^{-1} of LHCb data assuming a supersymmetric model. The dashed blue line shows the distribution taken as input, while the solid red line is the median of a thousand toy fits. The SM theoretical distributions are also shown with the same colour scheme as in Fig. 1. These two distributions must be statistically distinguishable if an observation of NP is to be made.

robust sign of NP. Furthermore, the transformation of some parts of the angular distribution under T -parity means that q^2 integrated measurements can be made without separating the data into B and \bar{B} samples [14]. Fig. 6 shows some model independent predictions for the angular asymmetry A_8 defined in Ref. [7] and the estimated sensitivity to it using two independent full angular fits. It seems clear that more work is required before these sort of measurements become competitive for anything other than very large NP phases. In the case of a full angular analysis other more theoretically clean observables may also be considered [15].

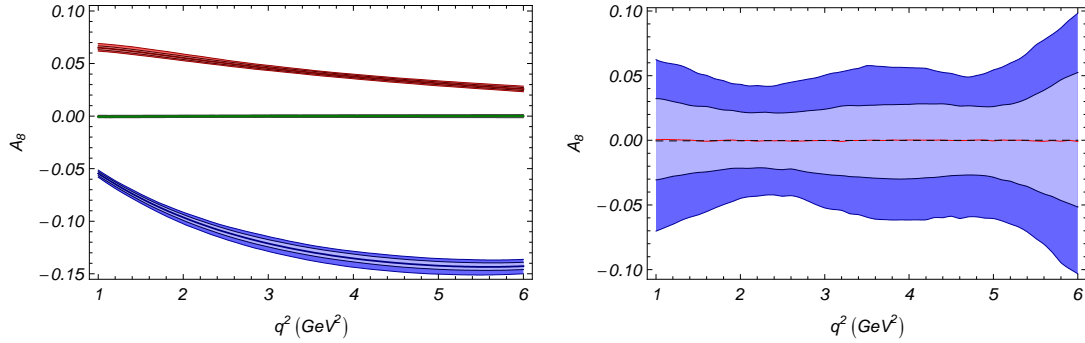


Figure 6: Left: Model independent distributions for the CP asymmetry in the angular component I_8 (A_8) for the SM (green) and NP with $\mathcal{C}_{9\text{NP}} = 2e^{i3\pi/4}$ (red), $\mathcal{C}_{10\text{NP}} = 2e^{i3\pi/4}$ (grey), and $\mathcal{C}_{10}^I = 3e^{i3\pi/4}$ (blue). The error bands show estimated Λ/m_b corrections [15] however other theoretical uncertainties are not shown. **Right:** Estimated experimental sensitivity to A_8 after performing two independent full angular fits to the B and \bar{B} samples assuming the SM for 10 fb^{-1} of LHCb data. The bands have the same meaning as in Fig. 5.

Acknowledgments

The author would like to thank the conference organisers for the convivial atmosphere created and also A. Bharucha, U. Egede, T. Hurth, J. Matias, and M. Ramon for many helpful discussions and stimulating collaborations.

References

- [1] **LHCb** Collaboration, A. A. Alves *et. al.*, *The LHCb Detector at the LHC*, *JINST* **3** (2008) S08005.
- [2] **BABAR** Collaboration, B. Aubert *et. al.*, *Angular distributions in the decays $B \rightarrow K^* l^+ l^-$* , *Phys. Rev.* **D79** (2009) 031102 [[0804.4412](#)]; **BELLE** Collaboration, J. T. Wei *et. al.*, *Measurement of the differential branching fraction and forward-backward asymmetry for $B \rightarrow K^{(*)} l^+ l^-$* , *Phys. Rev. Lett.* **103** (2009) 171801 [[0904.0770](#)].
- [3] U. Egede, T. Hurth, J. Matias, M. Ramon and W. Reece, *New observables in the decay mode $\bar{B}_d \rightarrow \bar{K}^{*0} \mu^+ \mu^-$* , *JHEP* **11** (2008) 032 [[0807.2589](#)].
- [4] U. Egede, “Angular correlations in the $\bar{B}_d \rightarrow \bar{K}^{*0} \mu^+ \mu^-$ decay.” [CERN-LHCb-2007-057](#).
- [5] A. Ali, T. Mannel and T. Morozumi, *Forward backward asymmetry of dilepton angular distribution in the decay $b \rightarrow sl^+ l^-$* , *Phys. Lett.* **B273** (1991) 505–512.
- [6] M. Beneke, T. Feldmann and D. Seidel, *Systematic approach to exclusive $B \rightarrow Vl^+ l^-$, $V\gamma$ decays*, *Nucl. Phys.* **B612** (2001) 25–58 [[hep-ph/0106067](#)]; M. Beneke, T. Feldmann and D. Seidel, *Exclusive radiative and electroweak $b \rightarrow d$ and $b \rightarrow s$ penguin decays at NLO*, *Eur. Phys. J.* **C41** (2005) 173–188 [[hep-ph/0412400](#)].
- [7] W. Altmannshofer *et. al.*, *Symmetries and asymmetries of $B \rightarrow K^{*0} \mu^+ \mu^-$ decays in the Standard Model and beyond*, *JHEP* **01** (2009) 019 [[0811.1214](#)].
- [8] A. Bharucha and W. Reece. In preparation.
- [9] J. Dickens, V. Gibson, C. Lazzeroni and M. Patel, “Selection of the decay $B_d \rightarrow K^{*0} \mu^+ \mu^-$ at LHCb.” [CERN-LHCb-2007-038](#); M. Patel and H. Skottowe, “A Fisher discriminant selection for $B_d \rightarrow K^{*0} \mu^+ \mu^-$.” [CERN-LHCb-2009-009](#).
- [10] **LHCb** Collaboration, B. Adeva *et. al.*, *Roadmap for selected key measurements of LHCb*, [0912.4179](#).
- [11] A. Ali, P. Ball, L. T. Handoko and G. Hiller, *A comparative study of the decays $B \rightarrow (K, K^*) l^+ l^-$ in Standard Model and supersymmetric theories*, *Phys. Rev.* **D61** (2000) 074024 [[hep-ph/9910221](#)].
- [12] J. Dickens, V. Gibson, C. Lazzeroni and M. Patel, “A study of the sensitivity to the forward-backward asymmetry in $B_d \rightarrow K^{*0} \mu^+ \mu^-$ decays at LHCb.” [CERN-LHCb-2007-039](#).
- [13] F. Kruger and J. Matias, *Probing new physics via the transverse amplitudes of $B^0 \rightarrow K^{*0} (\rightarrow K^- \pi^+) l^+ l^-$ at large recoil*, *Phys. Rev.* **D71** (2005) 094009 [[hep-ph/0502060](#)]; E. Lunghi and J. Matias, *Huge right-handed current effects in $B \rightarrow K^* (K\pi) l^+ l^-$ in supersymmetry*, *JHEP* **04** (2007) 058 [[hep-ph/0612166](#)].

- [14] C. Bobeth, G. Hiller and G. Piranishvili, *CP asymmetries in $\bar{B} \rightarrow \bar{K}^{*0}(\rightarrow \bar{K}\pi)l^+l^-$ and untagged $\bar{B}_s, B_s \rightarrow \phi(\rightarrow K^-K^+)l^+l^-$ decays at NLO*, *JHEP* **07** (2008) 106 [[0805.2525](#)].
- [15] U. Egede, T. Hurth, J. Matias, M. Ramon and W. Reece, “New physics reach of the mode $B_d \rightarrow K^*l^+l^-$: *CP* violating observables.” Talk at [EPS](#), 16.-22.7.2009, Krakow, Poland; U. Egede, T. Hurth, J. Matias, M. Ramon and W. Reece, “The exclusive $B_d \rightarrow K^*l^+l^-$ decay: *CP* violating observables.” Talk at [FLAVIANet](#), 23.-27.7.2009, Kazimierz, Poland; U. Egede, T. Hurth, J. Matias, M. Ramon and W. Reece. In preparation.